12

300 m
1000 ft

1000 m
3333 ft

2000 m
6666 ft

3000 m
9990 ft

DEEP OFFSHORE TECHNOLOGY

d.o.t.

1983

DEEP OFFSHORE TECHNOLOGY

2nd International Conference and Exhibition

17/19 October 1983

Mediterranean Conference Centre

Valletta
MALTA

PROCEEDINGS

III. NEW CONCEPTS OF PRODUCTION MEANS

J.E.W. Wichers and H.J.J. van den Boom
Project Manager Scientific Officer
Ocean Engineering Division Research and Development Division

Maritime Research Institute Netherlands (NSMB)

"Simulation of the Behaviour of SPM-moored Vessels in Irregular Waves, Wind and Current"

ABSTRACT

Vessels moored in the open sea are often used as storage, production and export loading facilities. Nowadays even in relatively deep water single point type mooring systems are frequently used. Due to the second order wave drift forces and possible instabilities of the system in current and wind, the vessel often shows large amplitude motions in the horizontal plane. Furthermore, the well known wave frequency motions are present in six degrees of freedom. Both components of motion may be responsible for high loads in the mooring system.

In early design stages of such systems, mathematical models can provide estimates of motions and mooring loads for various alternative configurations and environmental conditions. In this paper a general computer model for a time domain description of combined high and low frequency motions of SPM-moored vessels is presented. The instantaneous first and second order wave forces are computed from frequency domain results, the wave field description and the actual position of the vessel. Fluid reactive forces for arbitrary motions at wave frequencies are taken into account by convolution integrals. For the low frequency components a formulation is given describing the hydrodynamic interaction between the vessel and the current field.

Results of the current force formulation are compared with model test results. Moreover, results are given of the first step of an extensive validation in which outputs of computational simulations were compared to model test results. The comparisons, which were made for a tanker moored to a monopile by means of a bow hawser, show a good correlation for both motions and mooring forces.

INTRODUCTION

With the increase of size in Single Point Mooring systems, more attention has to be given to the mechanism of motions and structural forces both in the design stage and during the operational lifetime of such systems. The behaviour of a vessel moored to an SPM system in wind, waves and current (Fig. 1) is determined to a large extent by the slow motions of the tanker in the horizontal plane. Due to this behaviour, a slowly varying force is generated in the mooring system. Superimposed on this force are the wave frequency forces caused by buoy, tower or riser system and the vessel motions in six degrees of freedom. The combination of these forces may lead to high peak loads in the mooring system.

A mathematical approach to describe both motions and mooring forces is hampered by the non-linearities in both hydromechanics and mooring system. Moreover, large variations in heading strongly affect the environmental loading (Fig. 2).

Wichers [1] derived a mathematical model for small displacements around the equilibrium position of a bow hawser type mooring system under influence of wind and current only. The purpose of this model was to judge the dynamic stability and the natural frequencies of the moored tanker in the horizontal plane. It was found that under certain conditions the system was unstable, which means that large amplitude low frequency motions and mooring forces can be induced even in the absence of oscillatory exciting forces.

Whether the system is stable or unstable, if it is moored in irregular waves which give rise to low frequency wave drift forces, low frequency motions and mooring forces will be induced which will be resonant and, if the system damping is small, of large amplitudes. Therefore, before introducing low frequency wave drift forces in a theoretical model, it is necessary to develop a large motion amplitude mathematical model for wind and current only. A proper time domain description of the low frequency fluid reactive forces including viscous effects is essential. In the past several authors [2], [3], [4] and [5] have presented such formulations. In this paper a formulation will be used which is based on experimental model data. Comparisons with existing theories will be made.

When considering the six degrees of freedom of the moored vessel, not only the low frequency fluid reactive forces have to be accounted for but also the hydromechanic reaction forces in the wave frequency region. It is well known that these forces, often referred to as added mass and damping, are frequency dependent. The present paper describes a convolution method to incorporate these effects.

Due to the large horizontal motions of the vessel, wave forces not only depend on the encountered wave field but also on the instantaneous position and orientation of the vessel (Fig. 2). This paper describes the use of impulse response techniques to obtain first and second order wave forces in six degrees of freedom taking into account these aspects.

In the development of large computer simulation models regular verifications and try outs are indispensable. For this purpose model tests with a 200 kTDW tanker were carried out (Fig. 1). At the end of this paper several simulation results are compared with these model test results.

SIMULATION MODEL

Equations of motion

Considering the moored vessel as a linear mass-damper-spring system, according to Newton's law the equations of motion will have the following form:

$$\underline{A}\ddot{\underline{x}} + \underline{B}\dot{\underline{x}} + \underline{C}\underline{x} = \underline{F} \qquad \ldots\ldots\ldots\ldots\ldots\ldots (1)$$

For free-floating ships and barges in regular waves this formulation often leads to acceptable results when applied in the frequency domain. For moored structures application of equation (1) is hampered by the frequency dependency of A and B, and non-linearities in both fluid excitation and reactive forces. Moreover, the relationship between displacements of the vessel and the restoring forces due to the mooring system will not be linear. To overcome these difficulties it is assumed that excitation due to wind and waves can be separated from the motion mechanism in current.

The ultimate motions of the vessel will show components with wave frequencies and low frequency horizontal motions. It is well known that the former components are proportional to the wave height and mainly from potential origin, while the latter are non-linear and

dominated by viscous effects. For this reason the fluid reactive forces will be split up into low and high frequency contributions.

To describe the separate contributions in the equations of motion, use will be made of the two systems of co-ordinates presented in Fig. 3. The global right-handed system $O\text{-}x_1\text{-}x_2\text{-}x_3$ is earth-bound, defined with the positive x_3-axis vertically upwards. The local system is the global system translated to the low frequency centre of gravity and rotated to the low frequency horizontal orientation of the vessel.

When large rotations are present in the yaw mode of motion only, the relation between both systems is given by:

$$\underline{x} = T\,\underline{x}_B + \underline{x}_{COG} \qquad \ldots\ldots\ldots\ldots\ldots\ldots (2)$$

where:

$$T = \begin{pmatrix} \cos\psi & -\sin\psi & 0 & 0 & 0 & 0 \\ \sin\psi & \cos\psi & 0 & 0 & 0 & 0 \\ 0 & 0 & 1 & 0 & 0 & 0 \\ 0 & 0 & 0 & 1 & 0 & 0 \\ 0 & 0 & 0 & 0 & 1 & 0 \\ 0 & 0 & 0 & 0 & 0 & 1 \end{pmatrix} \quad \text{and} \quad \underline{x}_{COG} = \begin{pmatrix} X \\ Y \\ 0 \\ 0 \\ 0 \\ \psi \end{pmatrix} \qquad \ldots\ldots (3)$$

$\underline{x}_B$ is defined in the body system
$\underline{x}$ is defined in the global system
ψ is low frequency yaw.

Low frequency fluid reactive forces including current loads

The equations of horizontal low frequency motions of a free-floating vessel in current can be given in the body-bound system:

$$M(\ddot{\underline{x}}_B(t) + D\dot{\underline{x}}_B(t)) = F_{current}(\dot{\underline{x}}_B, \underline{x}_B, t) \qquad \ldots\ldots\ldots\ldots (4)$$

where: $$D = \begin{pmatrix} 0 & 0 & -\dot{x}_B(2) \\ 0 & 0 & \dot{x}_B(1) \\ 0 & 0 & 0 \end{pmatrix} \quad \text{and} \quad \underline{F}_c = \begin{pmatrix} F_c(1) \\ F_c(2) \\ F_c(6) \end{pmatrix}$$

and $$M = \begin{pmatrix} M_{11} & 0 & 0 \\ 0 & M_{22} & 0 \\ 0 & 0 & M_{66} \end{pmatrix}$$

The relative velocity of the vessel with respect to the fluid is:

$$\dot{V}_{cr} = (u_r^2 + v_r^2)^{\frac{1}{2}} \qquad \ldots\ldots\ldots\ldots\ldots\ldots (5)$$

in which: $u_r = \dot{x}_B(1) - V_c \cos(\alpha_c - \psi)$
$v_r = \dot{x}_B(2) - V_c \sin(\alpha_c - \psi)$
V_c = current velocity
α_c = current direction
ψ = yaw angle in global co-ordinates.

If the low frequency motions are small it can be assumed that the disturbances of the free fluid surface are negligible. Assuming that viscous effects are absent as well, Norrbin [6] derived:

$$F_c(1) = -\hat{M}_{11}\,\dot{u}_r + \hat{M}_{22}\,v_r\,\dot{\psi} + m_{26}\,\dot{\psi}^2 \qquad \ldots\ldots (6)$$

$$F_c(2) = -\hat{M}_{22}\,\dot{v}_r - \hat{M}_{11}\,u_r\,\dot{\psi} - m_{26}\,\ddot{\psi} \qquad \ldots\ldots (7)$$

$$F_c(6) = -\hat{M}_{66}\,\ddot{\psi} - (\hat{M}_{22} - \hat{M}_{11})u_r\,v_r - m_{62}(\dot{v}_r + u_r\,\dot{\psi}) \qquad \ldots\ldots (8)$$

where: m_{kj} = added mass coefficients at low frequency.

Equations (6) and (7) lead to the well known d'Alembert paradox because the right-hand sides are equal to zero for $\dot{u}_r = \dot{v}_r = \dot{\psi} = 0$. In equation (8) the term $(m_{22} - m_{11})u_r v_r$ is the only arising in an ideal fluid and often referred to as the Munk-moment.

In agreement with ship manoeuvring theories it may be assumed that inertia terms in the equations of motion are hardly affected by viscosity. Therefore equations (6) through (8) may be rewritten to:

$$F_c(1) = - m_{11} \bar{x}_B(1) + H(1)$$

$$F_c(2) = - m_{22} \bar{x}_B(2) - m_{26} \bar{\dot{\psi}} + H(2)$$

$$F_c(6) = - m_{66} \bar{\dot{\psi}} - m_{62} \bar{x}_B(2) + H(6) \qquad \ldots\ldots\ldots\ldots\ldots\ldots (9)$$

in which: $\underline{H} = H(\underline{V}, \psi, \dot{\psi})$

The functions H(2) and H(6) have been experimentally determined for a 200 kTDW tanker. To this end the vessel was towed with a constant speed while a steady rotation around the vertical axis $G\text{-}x_B(3)$ was applied. In this way low frequency fluid reactive forces were obtained for a range of relative current speeds, yaw velocities, loading conditions and water depths. For each water depth and loading condition the results can be expressed in terms of Fourier series, assuming $V_{cr} >> |\dot{\bar{x}}_B|$:

$$H(2) = \left\{ \tfrac{1}{2} C_0(2) + \sum_{n=1}^{N} C_n(2) \cos(n \alpha_{cr}) + S_n(2) \sin(n \alpha_{cr}) \right\} .$$

$$. \tfrac{1}{2} \rho_w L T V_{cr}^2 \qquad \ldots\ldots\ldots\ldots\ldots\ldots (10)$$

$$H(6) = \left\{ \tfrac{1}{2} C_0(6) + \sum_{n=1}^{N} C_n(6) \cos(n \alpha_{cr}) + S_n(6) \sin(n \alpha_{cr}) \right\} .$$

$$. \tfrac{1}{2} \rho_w L^2 T V_{cr}^2 \qquad \ldots\ldots\ldots\ldots\ldots\ldots (11)$$

where: $\alpha_{cr} = \arctan(v_r/u_r)$
$C_n = C_n(\dot{\psi}L/V_{cr})$

For the longitudinal motion of the vessel the following formulation is proposed:

$$H(1) = \tfrac{1}{2} \rho_w L T \{ C_x(\alpha_{cr}) V_c^2 - 2C_x(0) V_c \dot{\bar{x}}_B(1) \} \qquad \ldots\ldots (12)$$

where C_x is an empirical function of the relative current direction.

The formulations outlined above have been compared to the theory presented by Gerritsma et al [7]. This theory concerns deep water and a fully loaded vessel at even keel. The model distinguishes three contributions to the overall flow:

(i) ideal incompressible flow
(ii) viscous cross flow perpendicular to the longitudinal axis of the ship
(iii) lift forces generated by viscosity.

The ideal flow contribution corresponds to equations (6) through (8). The cross flow components can be formulated as:

$$F_{cf}(2) = - \tfrac{1}{2} \rho_w T C_{90}(2) \int_{-\frac{1}{2}L}^{\frac{1}{2}L} (v_r + \dot{\psi}x) |v_r + \dot{\psi}x| \, dx \qquad \ldots (13)$$

$$F_{cf}(6) = - \tfrac{1}{2} \rho_w T C_{90}(2) \int_{-\frac{1}{2}L}^{\frac{1}{2}L} |(v_r + \dot{\psi}x) |v_r + \dot{\psi}x|| x \, dx \qquad \ldots (14)$$

The lift contribution can be approximated by:

$$F_L(2) = -K \rho_w \pi T^2 \{|u_r| v_r + x_{c1} L u_r \dot{\psi}\} \quad \ldots\ldots\ldots (15)$$

$$F_L(6) = -K \rho_w \pi T^2 L\{x_{c1} u_r v_r + x_{c2}{}^2 L|u_r|\dot{\psi}\} \quad \ldots\ldots\ldots (16)$$

in which: K = empirical coefficient for low aspect ratio
x_{c1} = dimensionless centre connected to the distribution of the first moment of viscous force
x_{c2} = dimensionless centre connected to the distribution of the second moment of viscous force.

The coefficients K, x_{c1} and x_{c2} are presented as functions of B/L in Fig. 4.

Wave frequency fluid reactive forces

To account for the frequency dependent potential fluid reactive forces (i.e. damping and added mass) use can be made of the impulse response technique. This technique which is based on the linearity of the fluid reactions, describes the response to an arbitrarily varying force F(t) when the response R(t-τ) (retardation function) to a unit impulse at the time t=τ, is known:

$$x(t) = \int_{-\infty}^{t} F(\tau)\, R(t-\tau) d\tau \quad \ldots\ldots\ldots\ldots\ldots\ldots (17)$$

The impulse response theory has been used by Cummins [8] to formulate the fluid reactive forces due to ship motions by considering the vessel's velocity as system input and the reaction forces as output. The equations of motion in the time domain, derived within potential theory, obtained in this way, have the following form:

$$\sum_{j=1}^{6} (M_{kj} + m_{kj})\ddot{x}_j + \int_{-\infty}^{t} R_{kj}(t-\tau)\, \dot{x}_j(\tau) d\tau + C_{kj}\, x_j = F_k(\underline{x},\dot{\underline{x}},\ddot{\underline{x}},t) \quad \ldots\ldots\ldots\ldots\ldots\ldots (18)$$

where: x_j = motion in j-direction
$F_k(\underline{x},\dot{\underline{x}},\ddot{\underline{x}},t)$ = arbitrary in time varying forces in the k-mode of motion
M_{kj} = inertia matrix
C_{kj} = matrix of hydrostatic restoring forces
R_{kj} = matrix of retardation functions
m_{kj} = added inertia matrix.

The only basic assumption according to Cummins' formulation, viz. the separate treatment of the linear potential fluid reactive forces and all other forces, may be justified by known experimental techniques and numerical computations. This formulation allows non-linear restoring forces, frequency dependent linear fluid reactive forces, arbitrary excitation and interaction effects between low and high frequency behaviour. Hence, this approach is suitable for simulation of non-steady-state and transient motions of moored floating structures.

The right-hand side of equation (18) consists of relative current forces, wave loads, wind loads and mooring forces:

$$\underline{F}(\underline{x},\dot{\underline{x}},\ddot{\underline{x}},t) = \underline{F}_c(\underline{x},\dot{\underline{x}},\ddot{\underline{x}},t) + \underline{F}_{wave}(\underline{x},t) + \underline{F}_{wind}(\underline{x},\dot{\underline{x}},t) + \underline{F}_{moor}(\underline{x},t) \quad \ldots\ldots\ldots\ldots\ldots\ldots (19)$$

Computation of the left-hand side of equation (18) requires the total inertia, the hydrostatic coefficients and the retardation functions. Unfortunately, it is not practical to derive this input in the time domain directly, neither by measurements nor by computations. However, it is known that this information can be derived from frequency domain results.

The retardation function can be found from the damping curve over the complete range of frequencies:

$$R_{kj}(t) = \frac{2}{\pi} \int_0^{\infty} b_{kj}(\omega) \cos \omega t \, d\omega \qquad \ldots\ldots\ldots\ldots\ldots\ldots (20)$$

The inertia coefficient can be derived from the retardation function and the added mass at one frequency:

$$m_{kj} = a_{kj}(\omega) + \frac{1}{\omega} \int_0^{\infty} R_{kj}(\tau) \sin(\omega\tau) \, d\tau \qquad \ldots\ldots\ldots\ldots (21)$$

For the present study added mass and damping were computed by the program DIFFRAC. This program describes the 3-D potential flow by pulsating sources representing the vessel's hull.

Based on potential theory, this procedure obviously does not account for any viscous effects. Its application is shown by Van Oortmerssen [9].

Wave loads

As stated before, wave exciting loads are functions of the vessel's position and time. For a long-crested irregular wave train $\zeta_0(t)$ defined at a fixed position, the wave loads on a structure moving near this position may be formulated as:

$$F(\underline{x},t) = F^{(1)}(\underline{x},t) + F^{(2)}(\underline{x},t) \qquad \ldots\ldots\ldots\ldots (22)$$

$$F^{(1)}(\underline{x},t) = \int_0^{\infty} g^{(1)}(\psi,\tau) \, \zeta(\underline{x},t-\tau) d\tau \qquad \ldots\ldots\ldots\ldots (23)$$

$$F^{(2)}(\underline{x},t) = \int_0^{\infty} \int_0^{\infty} g^{(2)}(\psi,\tau_1,\tau_2) \, \zeta(\underline{x},t-\tau_1) \, \zeta(\underline{x},t-\tau_2) d\tau_1 d\tau_2 \quad \ldots (24)$$

The local wave elevation ζ may be obtained from ζ_0:

$$\zeta(\underline{x},t) = \int_0^{\infty} w(\underline{x},\tau) \, \zeta_0(t-\tau) d\tau \qquad \ldots\ldots\ldots\ldots\ldots (25)$$

$$\text{with:} \quad w(\underline{x},\tau) = \frac{1}{2\pi} \int_{-\infty}^{\infty} W(\omega) \, e^{i\omega\tau} \, d\omega \qquad \ldots\ldots\ldots\ldots (26)$$

$$\text{and :} \quad W(\omega) = \frac{\zeta(\underline{x},\omega)}{\zeta_0(\omega)} \qquad \ldots\ldots\ldots\ldots\ldots (27)$$

It should be noted that this transformation of wave elevations is only valid for neighbouring locations.

The linear and quadratic kernels $g^{(1)}$ and $g^{(2)}$ are found from the Fourier transform of the corresponding frequency domain transfer functions:

$$g^{(1)}(\psi,\tau) = \frac{1}{2\pi} \int_{-\infty}^{\infty} G^{(1)}(\psi,\omega) \, e^{-i\omega\tau} \, d\omega \qquad \ldots\ldots\ldots (28)$$

$$g^{(2)}(\psi,\tau_1,\tau_2) =$$

$$= \frac{1}{(2\pi)^2} \int_{-\infty}^{\infty} \int_{-\infty}^{\infty} G^{(2)}(\psi,\omega_1,\omega_2) \, e^{-i(\omega_1\tau_1 + \omega_2\tau_2)} \, d\omega_1 d\omega_2 \qquad \ldots (29)$$

For all six degrees of freedom the first order wave force transfer functions $G^{(1)}$ were obtained from the computer program DIFFRAC. The quadratic transfer functions $G^{(2)}$ were computed according to the direct pressure integration method developed by Pinkster [10]. Both transfer functions are defined in the body system of co-ordinates, hence the instantaneous wave direction only includes the low frequency yaw component ψ.

This component may be approximated from:

$$\psi(t) = \int_0^{\infty} L(\tau)\, x(6)(t-\tau)d\tau \qquad \ldots\ldots\ldots\ldots\ldots\ldots (30)$$

with $L(\tau)$: causal filter.

The formulation given above is an extension to the method for small amplitude motions presented by Pinkster and Huijsmans [11].

Wind loads

For the wind forces and moments relative to the tanker-bound system of co-ordinates, use is made of the relative motion concept described in [2].

Mooring

Forces due to the mooring are provided by a bow hawser or a yoke connection. These forces consist of restoring components due to excursions of the tanker bow, environmental loading of the mooring and sometimes the mooring dynamics. In general, hydromechanical interactions are negligible.

Dynamics of the mooring system normally do not affect the behaviour of the moored vessel because of the differences in mass and natural frequencies. For that reason it is sufficient to use the load-excursion characteristics of the total system in still water when simulating the behaviour of the vessel.

To derive the mooring loads, the possible dynamics of the mooring system can be superimposed, taking into account the simulated bow motions of the vessel.

Computational procedures

Having defined all models of the separate terms in the equations of motion, the computational scheme to be followed during the time domain simulation is presented in Fig. 5.

Knowing the time histories of excursions and their time derivatives in the global system all these values acting on the vessel have to be computed for the next simulation time step. The transformation of the body co-ordinates into global co-ordinates is given by equation (2):

$$\underline{x} = T\,\underline{x}_B + \underline{x}_{COG} \qquad \ldots\ldots\ldots\ldots\ldots\ldots (2)$$

The wave frequency fluid reactive forces may be calculated from the vessel's velocity in the local system, which can be found from:

$$\dot{\underline{x}}_B = T^{-1}(\underline{x} - \underline{x}_{COG}) + T^{-1}(\dot{\underline{x}} - \dot{\underline{x}}_{COG}) \qquad \ldots\ldots\ldots\ldots (31)$$

Together with the global orientation of the vessel and the wind and current direction and velocities, equation (31) is input for the wind and current model.

The global low frequency position and orientation of the vessel are also used to transform the wave record into wave forces.

Global mooring forces $\underline{F}(\underline{x},t)$ are found from the global displacements of the vessel and load-excursion characteristics of the mooring system. Mooring forces in the body system $\underline{F}_B(\underline{x},t)$ follow from:

$$\underline{F}_B(\underline{x},t) = T^{-1}\,\underline{F}(\underline{x},t) \qquad \ldots\ldots\ldots\ldots\ldots\ldots (32)$$

Knowing all loads in the local system, the accelerations of the vessel are solved in these co-ordinates and then transformed to the

global system:

$$\underline{\ddot{x}} = \bar{T}\,\underline{x}_B + 2\dot{T}\,\underline{\dot{x}}_B + T\,\underline{\ddot{x}}_B + \underline{\ddot{x}}_{COG} \qquad \ldots\ldots\ldots\ldots (33)$$

Finally, the global velocities and displacements are derived by numerical integration.

MODEL TESTS

General

Model tests were carried out to obtain empirical coefficients used in the low frequency relative current formulation and to verify the simulation procedures and numerical techniques.

The tests were carried out at a scale of 1 to 82.5 on basis of Froude's law of similitude. The model representing the 200 kTDW tanker was fitted with a superstructure aft and equipped with a non-active propeller and rudder. A body plan and the main particulars of the tanker are given in Fig. 6.

The bow hawser consisted of a thin steel wire running from the fixed terminal point through the bow fairlead. On the foredeck of the model a spring system was installed representing the non-linear hawser characteristics (Fig. 7).

Yaw rotating tests

In order to determine the low frequency reactive forces in current, yaw rotating tests were carried out in the Shallow Water Laboratory of MARIN. This basin measures 16 m by 220 m and is provided with a towing carriage. The water depth amounted to 1 m. Connected to the carriage is a yaw shaft which can be rotated at an adjustable speed. The shaft was connected to ship-bound transducers in line with the centre of gravity of the tanker. A typical result of these tests is given in Fig. 8.

SPM model tests

The SPM model tests were carried out in the Wave and Current Laboratory of MARIN, which measures 40 m by 60 m. The water depth amounted to 1 m. A review of the environmental conditions applied during the tests is given in Fig. 9. Wind was generated by portable wind fans. Fig. 10 shows the measured wave spectra while Fig. 11 presents the spectra of the square of the wave envelopes. The latter indicates the level of the wave drift forces.

After adjustment of current, wind and wave spectra the tanker was installed in the middle of the basin and moored by means of the hawser to a fixed point. The position of this point and the fairlead were in a horizontal plane in still water.

During the tests the motions at the fairlead were measured in an earth-bound system by an optical tracking device. The yaw angle was measured by an optical laser beam device while roll and pitch angles were recorded by means of gyroscopes. A strain-gauge transducer was used to measure the bow hawser tension.

RESULTS

Wind and current

The flow forces measured for the fully loaded tanker rotating with a constant yaw velocity of -0.003 rad/s in a 2 knot current is shown in Fig. 12. Results of the Fourier approximation (e.g. equations (10) and (11)) are given by a dotted line.

The results have been compared with the results of equations (6) through (8) and (13) through (16), (ref. [7]). For the cross flow formulation the resistance coefficient $C_{90}(2)$ was taken equal to 0.69. Lift coefficients were taken from Fig. 4. Added mass coefficients were computed by the program DIFFRAC.

From the results it can be concluded that a good agreement is found for $112.5° < \alpha_{cr} < 225°$. Outside this region the results are less satisfactory. This may be explained by the differences between the theoretical Munk-moment and the measured stationary yaw moment as shown in Fig. 12.

To validate the wind and current formulation excitation tests were carried out during the model tests and by computer simulations as well. The results are shown in Fig. 13.

Correlation tests

As a first step to validate the complete chain of theories and numerical techniques presented before, model tests and computer simulations were carried out for the 60 per cent loaded tanker in the environmental conditions shown in Fig. 9. These conditions yield stable motions with limited amplitudes of the tanker and therefore the effect of the low frequency horizontal motions is not taken into account in the calculation of wave forces. Wave force records were obtained directly from the undisturbed wave elevation measured at the location of the centre of gravity of the tanker, taking into account the mean horizontal orientation of the vessel.

This procedure enabled a direct comparison of the simulated and measured motions and mooring force records. Fig. 14 shows these records for environmental condition 2 (180° waves; 135° wind; 90° current). Good agreement is found in both amplitudes and phases. Figs. 15 and 16 present the results of spectral analysis for a duration of 6200 seconds. As illustrated by Figs. 17 and 18, for environmental condition 3 (180° waves; 180° wind; 90° current), the results were less satisfactory. Sway at the tanker bow was clearly underpredicted due to a small yaw motion in the simulation.

For environmental condition 1 (180° waves, wind and current) the surge motion (Fig. 19) is mainly responsible for the bow hawser tension (Fig. 20). From the comparison of sway and yaw it appeared that the effect of changes of wave direction, caused by variation of heading of the vessel, should be incorporated in the simulation.

Though of minor importance for this mooring system, the simulated vertical motions of the vessel corresponded to the measured values for all tests.

CONCLUSIONS

In this paper a mathematical approach to describe the behaviour of SPM-moored vessels is given. The empirical description of the low frequency vessel-current interactions provides a practical tool in the simulation of the non-linear low frequency fluid reactive forces. Impulse response techniques, using frequency domain wave force transfer functions as input, can be used to obtain the instantaneous first and second order wave forces for a given wave record. This enables the direct comparison of measured and simulated records of motions and mooring forces.

The first step of the correlation study yielded satisfactory results. More investigations will be carried out to validate the presented model with special attention to unstable situations of an SPM system.

NOMENCLATURE

A : matrix of inertia coefficients
B : matrix of damping coefficients
C : matrix of hydrostatic restoring coefficients, drag coefficient, Fourier coefficient
D : matrix
F : force (vector)
G : wave force transfer function
H : relative current force function
K : aspect ratio coefficient
L : causal filter
M : matrix of inertia
R : matrix of retardation functions, retardation function
T : matrix for local to global transformation, draft
V : velocity
W : wave train transfer function
X : low frequency longitudinal position of the centre of gravity
Y : low frequency transverse position of the centre of gravity

a : frequency dependent added mass
b : frequency dependent damping
c : current
cf : cross flow
g : impulse response function of wave forces
j : mode of motion
k : mode of motion
m : added inertia coefficient (matrix)
r : relative
t : time
u : longitudinal fluid velocity
v : transverse fluid velocity
w : impulse response function of wave transformation
$\underline{x}$: displacement vector (surge, sway, heave, roll, pitch, yaw)

α : angle of incidence
ζ : wave elevation
ρ_w : specific mass of water
τ : time
ψ : low frequency orientation of the vessel
ω : circular wave frequency

REFERENCES

[1] WICHERS, J.E.W.: "On the slow motions of tankers moored to single point mooring systems", Proc. 8th Offshore Technology Conference, OTC 2548, May 1976.

[2] WICHERS, J.E.W.: "Slowly oscillating mooring forces in single point mooring systems", Proc. BOSS'79, London, 1979.

[3] MOLIN, B. and BUREAU, G.: "A simulation model for the dynamic behaviour of tankers moored to SPM", Int. Symposium on Ocean Engineering and Ship Handling, Gothenburg, 1980.

[4] SORHEIM, H.R.: "Analysis of motion in single-point-mooring systems", Modelling Identification and Control, Vol. 1, No. 3, 1980.

[5] RATCLIFFE, A.T. and CLARKE, D.: "Development of a comprehensive simulation model of a single point mooring system", The Royal Institution of Naval Architects, Paper 9, London, 1980.

[6] NORRBIN, N.H.: "Theory and observations on the use of a mathematical model for a ship manoeuvring in deep and confined waters", Proc. 8th Symposium on Naval Hydrodynamics, 1970.

[7] GERRITSMA, J., BEUKELMAN, W. and GLANSDORP, C.C.: "The effect of beam on the hydromechanic characteristics of ship hulls", Proc. Symposium on Naval Hydrodynamics, Boston, 1974.

[8] CUMMINS, W.E.: "The impulse response function and ship motions ", DTMB Report 1661, Washingtion DC, 1962.

[9] OORTMERSSEN, G. VAN: "The motions of a moored ship in waves", NSMB Publication No. 510, 1976.

[10] PINKSTER, J.A.: "Low frequency second order wave exciting forces on floating structures", NSMB Publication No. 650, 1980.

[11] PINKSTER, J.A. and HUIJSMANS, R.H.M.: "The low frequency motions of a semi-submersible in waves", Proc. BOSS'82, Boston, 1982.

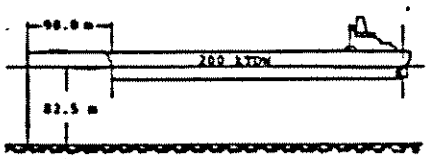

Fig. 1 SPM set-up for computations and model tests

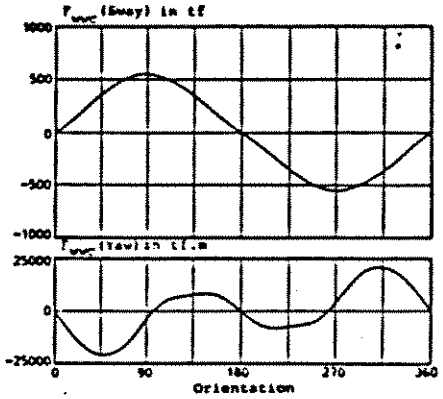

Fig. 2 Mean wind, wave and current forces

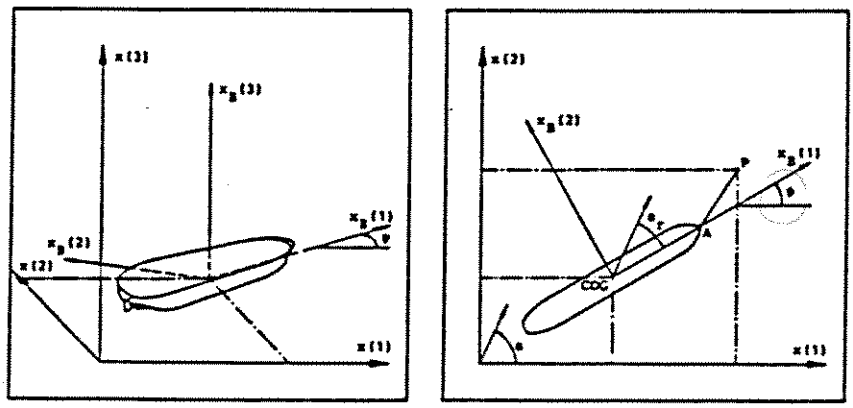

Fig. 3 Systems of co-ordinates

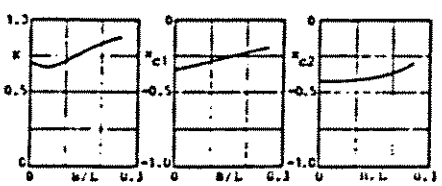

Fig. 4 Empirical coefficients for lift calculation, [7]

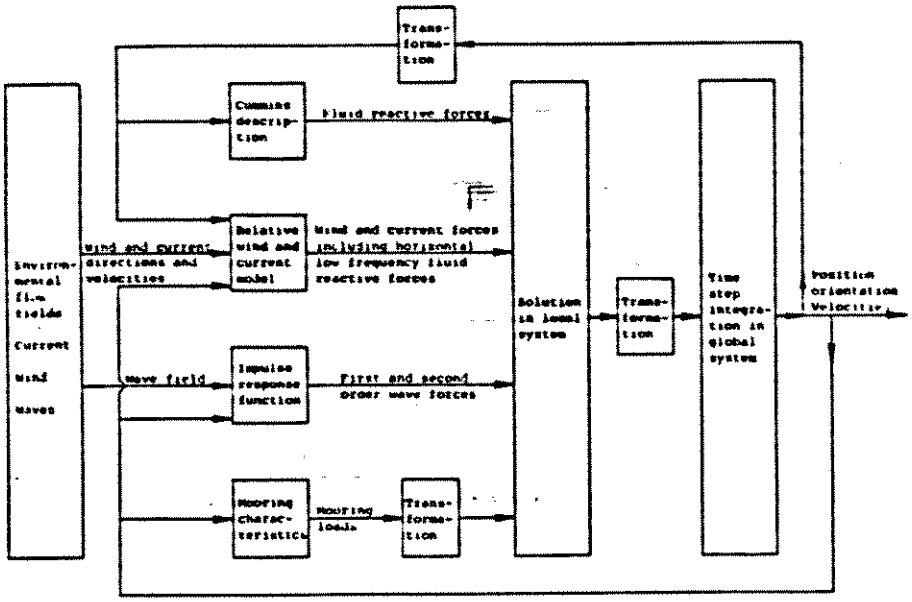

Fig. 5 Computational scheme for simulation

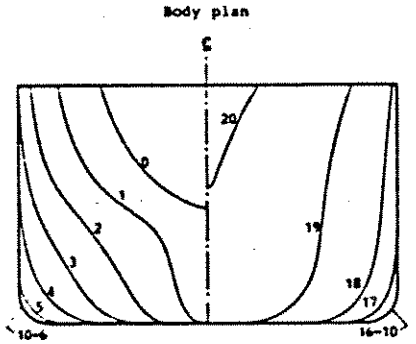

Designation	Symbol	Unit	200 kTDW tanker
Length between perpendiculars	L_{pp}	m	310.00
Breadth	B	m	47.17
Draft even keel (80% loaded)	T	m	13.23
Depth	H	m	29.70
Displacement volume	∇	m^3	159,698
Centre of gravity above keel	$\overline{KG}$	m	11.55
Metacentric height	$\overline{GM}$	m	8.66
Longitudinal radius of gyration	k_{yy}	m	77.55
Vertical radius of gyration	k_{zz}	m	83.81
Distance between centre of gravity and fore perpendicular	Lf	m	145.96
Lateral area of superstructure	A_{LS}	m^2	922
Frontal area of superstructure	A_{FS}	m^2	853

Fig. 6 Main particulars of tanker

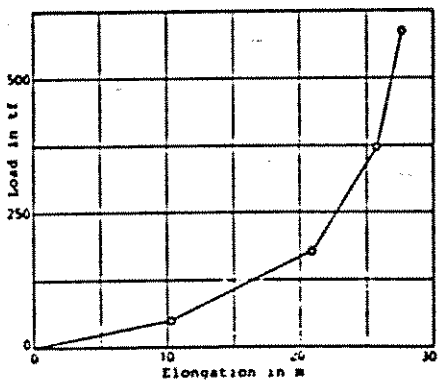

Fig. 7 Bow hawser load-elongation characteristic

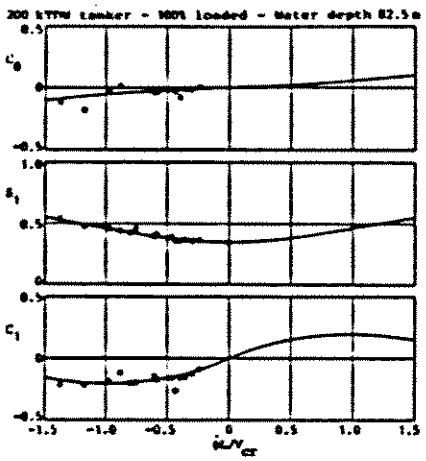

Fig. 8 Fourier coefficients for lateral force

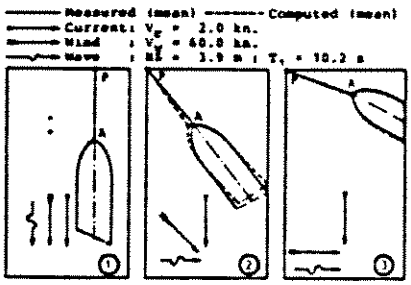

Fig. 9 Environmental conditions on the SPM system

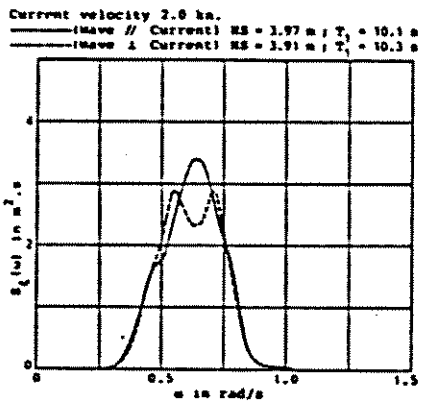

Fig. 10 Measured wave spectra

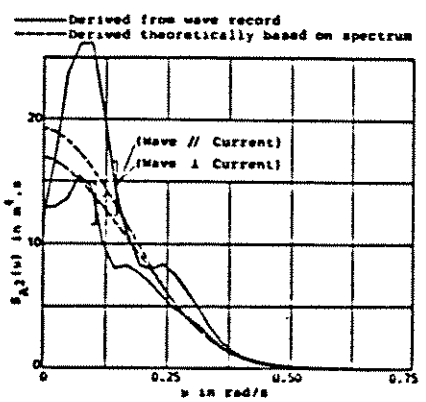

Fig. 11 Spectra of square of wave envelope

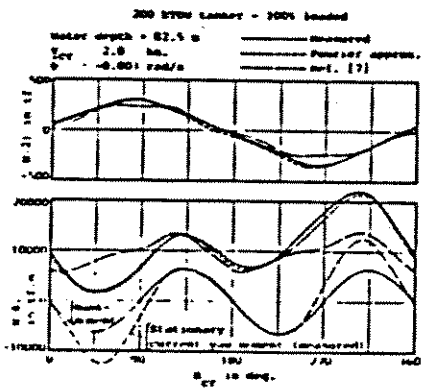

Fig. 12 Lateral current force and yaw moment

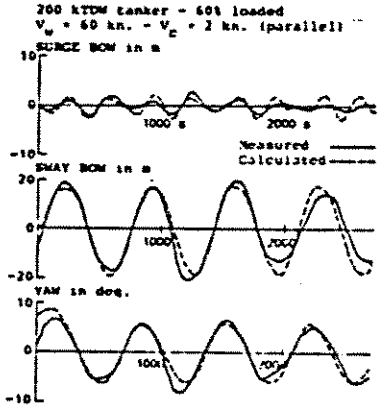

Fig. 13 Extinction tests

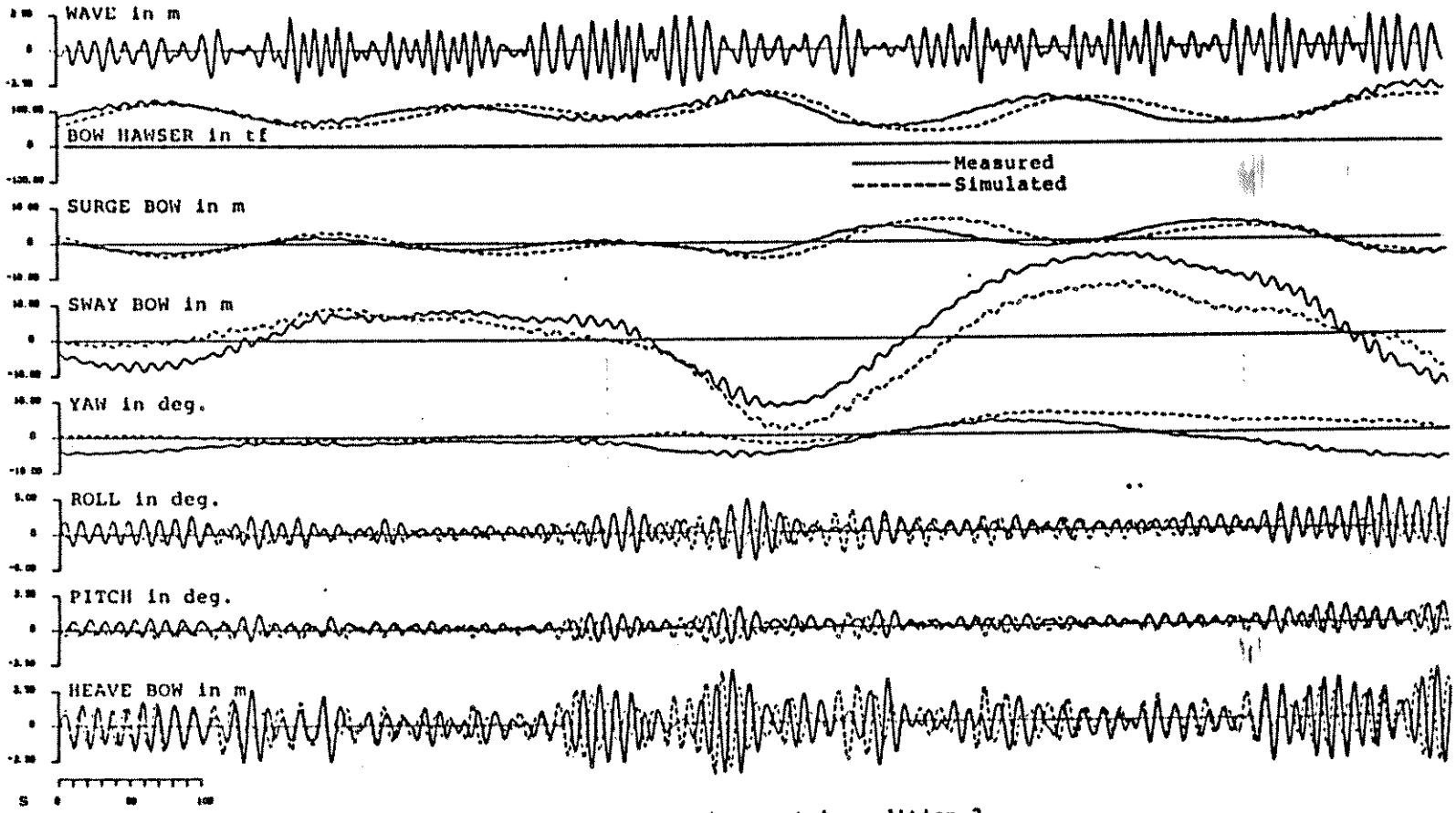

Fig. 14 Records of motion and bow hawser force for environmental condition 2

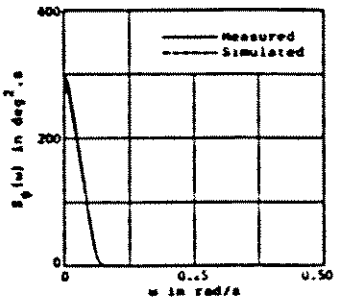

Fig. 15 Spectra of yaw (env. cond. 2)

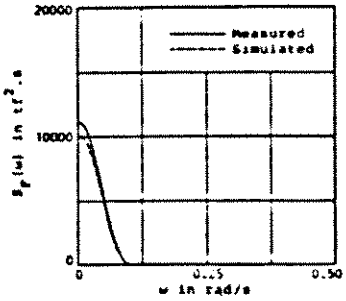

Fig. 16 Spectra of bow hawser force (env. cond. 2)

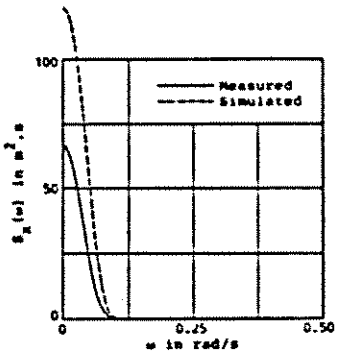

Fig. 17 Spectra of surge at bow (env. cond. 3)

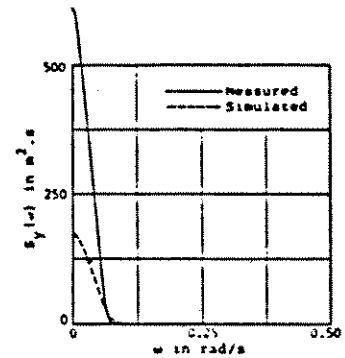

Fig. 18 Spectra of sway at bow (env. cond. 3)

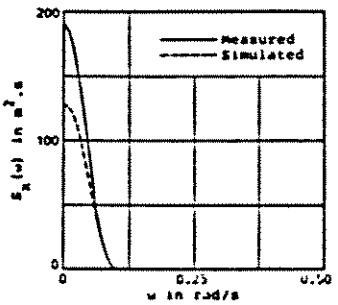

Fig. 19 Spectra of surge at bow (env. cond. 1)

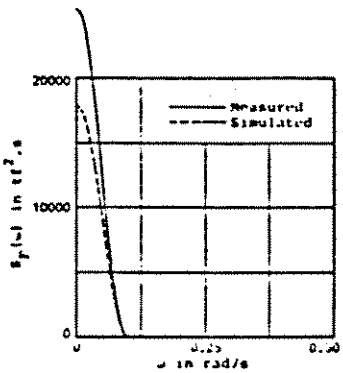

Fig. 20 Spectra of bow hawser force (env. cond. 1)